Phys. Status Solidi B **246**, No. 11–12, 2568–2571 (2009) / **DOI** 10.1002/pssb.200982331

physica status solidi b
www.pss-b.com
basic solid state physics

Current–phase relation in graphene and application to a superconducting quantum interference device

Çağlar Girit[1,2], Vincent Bouchiat[†,3], Ofer Naaman[†,4], Yuanbo Zhang[1], M. F. Crommie[1,2], A. Zettl[*,1,2], and Irfan Siddiqi[,1,4]**

[1] Department of Physics, University of California, Berkeley, California 94720, USA
[2] Materials Sciences Division, Lawrence Berkeley National Laboratory, Berkeley, California 94720, USA
[3] Institut Néel, CNRS/UJF, BP 166, 38042 Grenoble Cedex 9, France
[4] Quantum Nanoelectronics Laboratory, University of California, Berkeley, California 94720, USA

Received 28 May 2009, accepted 24 September 2009
Published online 18 November 2009

PACS 73.21.−b, 74.50.+r, 85.25.Cp, 85.25.Dq

[*] Corresponding author: e-mail azettl@berkeley.edu, Phone: 1 (510) 642-4939, Fax: 1 (510) 643-8793
[**] Corresponding author: e-mail irfan_siddiqi@berkeley.edu, Phone: 1 (510) 642-5620, Fax: 1 (510) 643-8497
[†] These authors contributed equally to the work.

Graphene exhibits unique electrical properties on account of its reduced dimensionality and neutrino-like "massless Dirac fermion" quasiparticle spectrum. When contacted with two superconducting electrodes, graphene can support Cooper pair transport, resulting in the well-known Josephson effect. The current–phase relation in a ballistic graphene Josephson junction is unique, and could provide a signature for the detection of ballistic Dirac fermions. This relation can be measured experimentally either directly via incorporation of graphene in an RF superconducting quantum interference device (SQUID) or indirectly via a dc-SQUID. We calculate the

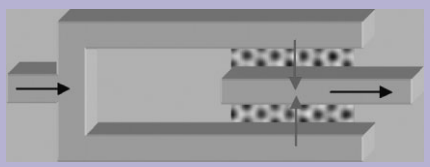

expected flux modulation of the switching current in the case of the dc-SQUID and compare the results to a previous experiment. Further experiments investigating the current–phase relation in graphene are promising for the observation of ballistic Dirac fermions.

1 Introduction Graphene, a two-dimensional allotrope of carbon extracted in 2004 [1], has many interesting electronic properties on account of its neutrino-like band structure [2]. The quasiparticles in graphene, called Dirac fermions, are massless with pseudo-spin half and have a linear energy–momentum dispersion relation. Many experiments on graphene seek to verify the existence of or probe the consequences of such a quasiparticle dispersion. One of the most common techniques is electronic transport measurements, and although results abound in the diffisuve regime [3], where the carrier mean free path is much shorter than the inter-electrode separation, there is no definitive data on transport of *ballistic* Dirac fermions. The problem inherent in diffusive electronic transport is that the combined system of quasiparticles *plus* scatterers is probed rather than just the quasiparticles themselves. The ballistic regime, in which there is no scattering, directly investigates the behavior of Dirac fermions. Unfortunately, this regime is currently much more difficult to access experimentally than the diffusive one despite advances in suspending devices [4, 5], which eliminates the strong contribution to scattering from the substrate. Nonetheless, most theoretical calculations or predictions for interesting graphene-based devices [6, 7] ignore scattering completely and are completely in the ballistic regime.

Here, following Titov et al. we calculate the expected transport parameters such as conductance in the ballistic case for the simplest device geometries. In addition to considering graphene contacted with normal metals, we present results for graphene Josephson junctions. Graphene as a weak link

in a superconducting loop is an interesting system to study since the magnetic flux threading the loop controls the phase difference across the junction and provides a complementary tuning knob to the electric field set by the back gate. The expected switching current dependence on magnetic flux for graphene in a ballistic dc superconducting quantum interference device (SQUID) is presented and compared to a previous experiment.

2 Transport calculations The Landauer formalism is used to calculate the conductance and current–phase relations for the graphene junction geometry described by Fig. 1. In the case of graphene, the transmission coefficients are calculated by solving the transmission problem for the Weyl equation instead of the Schroedinger equation, and one obtains:

$$T_n = \frac{k_n^2}{k_n^2 \cos^2 k_n L + k_F^2 \sin^2 k_n L} \tag{1}$$

where the n-th transverse mode has wavevector $q_n = (n + 1/2)\pi/W$, the Fermi wavevector is k_F, and $k_n^2 \equiv k_F^2 - q_n^2$ [8].

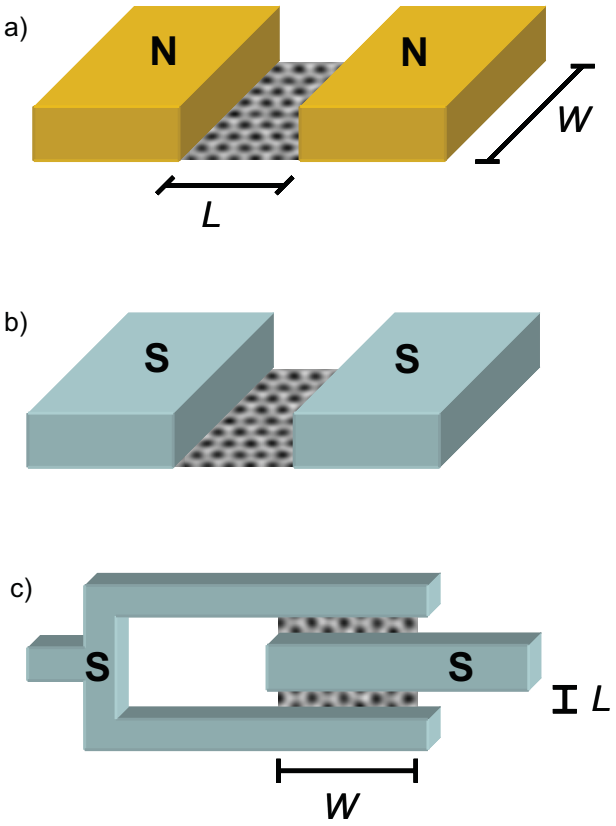

Figure 1 (online color at: www.pss-b.com) Device geometries: (a) graphene sandwiched between two normal metal electrodes (**N**). The electrode spacing is L and the width of the graphene sheet is W. (b) Graphene Josephson junction with superconducting electrodes (**S**). (c) dc graphene superconducting interference device, as employed in Ref. [4]. The phase difference across the junctions is controlled by the magnetic flux through the loop A.

The conductance $G = I/V$ for the graphene junction with normal metal contacts of Fig. 1a is given by the Landauer formula:

$$G = \frac{4e^2}{h} \sum_n T_n. \tag{2}$$

The graphene conductance quantum $4e^2/h$ includes both spin and valley degeneracy. The Fermi wavevector $k_F = \sqrt{\pi n}$ will vary as the square root of the back-gate voltage applied in a standard field-effect geometry ($n = cV_{gate}$, with c the capacitance per unit area). There is always some residual carrier density of order $10^{10}\,\mathrm{cm}^{-2}$ in unsuspended samples and $10^8\,\mathrm{cm}^{-2}$ in suspended ones due to charged impurities in the substrate in the first case and defects and/or adsorbates in the second. This will smear out the conductance near the Dirac point. However, in a geometry where $W \gg L$ and far from the Dirac point, we solve Eq. (2) and obtain a dependence $G \propto k_F$ and hence $G \propto \sqrt{V_{gate}}$. This sub-linear gate dependence with power one-half far from the Dirac point is a sign of ballistic conductance in wide and short samples, and contrasts with the linear gate dependence observed in diffusive samples in the long and narrow geometry. Other signs are a small oscillation on top of the square-root dependence whose spacing also varies as the square root of the gate voltage (not shown). The oscillation maxima occur at multiples of π/L and correspond to resonant transmission at the particle-in-a-box wavelengths.

For a superconductor–graphene–superconductor Josephson junction (Fig. 1b), one can likewise calculate the current–phase relation [8]:

$$I(\phi) = \frac{e\Delta_0}{\hbar} \sum_n \frac{T_n \sin(\phi)}{\sqrt{1 - T_n \sin^2(\phi/2)}} \tag{3}$$

which can be evaluated numerically and is plotted for several gate voltages in Fig. 2a for a wide-and-short device ($W \gg L$). The superconducting gap is Δ_0. We note several features: (1) φ_c, the phase which maximizes the critical current, oscillates by roughly 20° as a function of gate voltage; (2) much like in the normal case, the maximum critical current varies as the square root of the gate voltage far from the Dirac point and shows similar oscillations; (3) the product of the maximum critical current and the normal state resistance also shows oscillations as a function of gate voltage. All these features are signatures of ballistic transport in the wide-and-short geometry.

The current–phase relation can be directly measured by various techniques, one of which is by incorporating the graphene Josephson junction in an RF SQUID [9].

Given this current–phase relation, we can calculate the critical current variation as a function of magnetic field and gate voltage for the graphene dc SQUID of Fig. 1c. Ignoring any loop inductance, we maximize the sum $I(\phi + \theta) + I(\phi - \theta)$ over θ, where $\phi = 2\pi\Phi/\Phi_0$ and θ are the difference between and the sum of the phases of the two

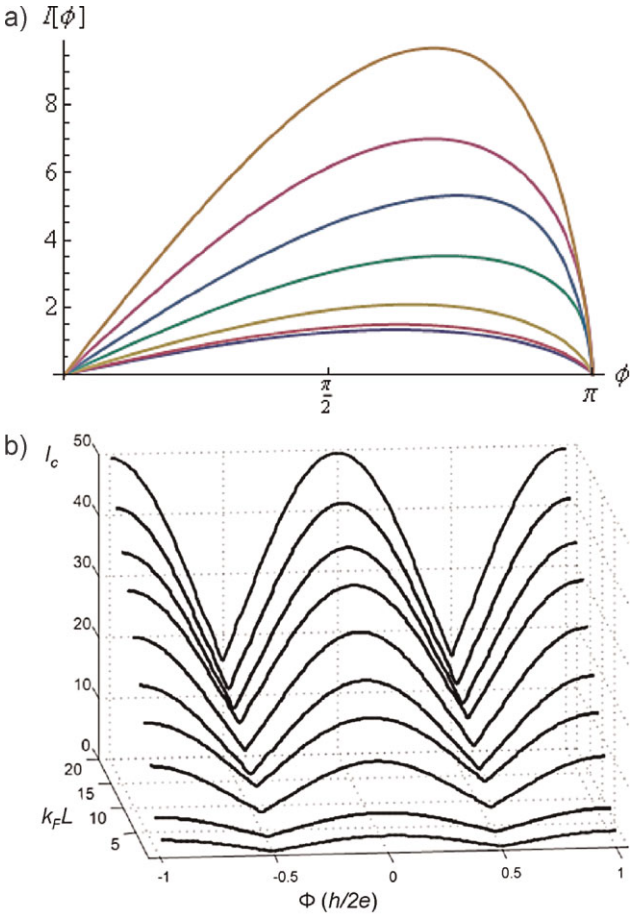

Figure 2 (online color at: www.pss-b.com) (a) Current–phase relation for a graphene Josephson junction with $W \gg L$ for several different values of the Fermi wavevector. From top to bottom $k_F L$ is 8, 6, 4, 3, 2, 1, and 0 (Dirac point). The critical current is given in units of $e\Delta_0 W/2hL$. (b) Critical current variation as a function of magnetic flux for the dc superconducting quantum interference device in Fig. 1c. Critical current is in arbitrary units.

Josephson junctions comprising the SQUID, respectively. The applied magnetic field H tunes the phase difference via the flux threading the SQUID loop of area A, $\Phi/\Phi_0 = HA/(h/2e)$. The resulting graph, Fig. 2b, shows that the modulation should be sinusoidal near the critical current maxima (constructive interference, $\Phi = n\Phi_0$) and triangular near the minima [destructive interference, $\Phi = (2n+1)\Phi_0/2$]. In addition, the critical current at the minima does not drop to zero, and full modulation is not expected at *any* gate voltage, including the Dirac point. Furthermore, calculation for the case of an asymmetric SQUID, where the Josephson energies of the two junctions are different, gives a skewed critical current–flux relationship. This reproduces the effect of an inductance in series with one of the junctions in the SQUID.

In the normal state, an ideal symmetric, ballistic graphene dc SQUID is two junctions as in Fig. 1a in parallel and should show twice the conductance calculated above, with $G \propto \sqrt{V_{\text{gate}}}$ and peaks at $k_F = n\pi/L$. Below the superconducting transition temperature of the contacts, the critical current as a function of gate voltage at zero flux should show behavior similar to the conductance in the normal state. The applied magnet field should also modulate the critical current as in Fig. 2b. All of these signatures together would be conclusive evidence for ballistic electronic transport in a single graphene device.

3 Experiment The present authors measured graphene dc SQUIDs in the geometry of Fig. 1c [10]. Typical junction width was several microns and junction length from 50 to 200 nm. The contacting Pd/Al electrodes (5/45 nm) themselves were 0.5 μm wide. This geometry is attractive because the properties of the graphene sheet, such as overall substrate doping, should be similar for the two junctions since they are so closely spaced. In addition, samples which are not rectangular can be used as long as the variation in sheet width is small relative to the junction spacing, roughly one micron. In order to approach the ballistic limit, high resolution electron beam lithography was used to define junction gaps as small as 50 nm. Although even smaller gaps could be patterned, liftoff was unsuccessful in that case. Even with 50 nm gaps however, the mean free path is at best comparable to L given our device mobilities.

Before patterning electrodes, the graphene is extracted from Kish graphite and deposited on degenerately doped p-type silicon wafers with 285 nm of silicon dioxide. Single layers are identified by analyzing optical contrast and confirmed with Raman spectroscopy. Devices are mounted in a dilution refrigerator with base temperature 20 mK and connected to highly filtered lines. A magnetic field perpendicular to the plane of the sample is applied by a small superconducting coil attached above the sample. The carrier density is varied by the back-gate voltage applied to the degenerately doped silicon layer.

Figure 3 shows measurements taken on a single graphene dc SQUID with $W/L \sim 20$ and $L \sim 80$ nm. The modulation of the mean switching current as a function of the applied magnetic field at several values of the gate voltage is given by the black dots. To make the measurements, multiple hysteretic IV curves are taken for a fixed value of the magnetic field and back-gate voltage. A histogram of the switching current is recorded and the mean value is plotted in Fig. 3. The curves are sinusoidal with slight skew indicative of a loop inductance.

They can be fit (solid lines) using the model of Fulton and Dynes [11] for a SQUID with asymmetric junctions and loop inductance. Assuming a sinusoidal current–phase relation appropriate for tunnel junctions, the skewness is fit by a small gate-voltage independent loop inductance parameter $2\pi L_0 I_0/\Phi_0 \sim 0.2$. The junction asymmetry ratio is given by the fits to be approximately 10:1 (ratio between the critical currents in each branch of the SQUID) and varies slightly with the gate voltage. Given the fitted value of the critical current of the stronger branch, I_0, we estimate the loop inductance L_0 to be on the order of 10 pH, comparable to an estimate of 15 pH obtained for a rectangular wire loop of the dimensions of our SQUID. Hence the skewness can be explained by the physical loop inductance, but the reason for the high

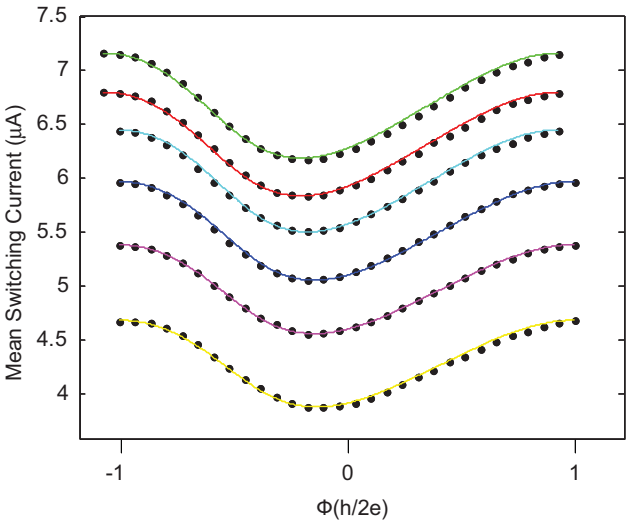

Figure 3 (online color at: www.pss-b.com) Measured mean switching current of a wide-and-short ($W \gg L$) graphene dc superconducting quantum interference device as a function of magnetic flux. Traces are at different gate voltages, with −25 V at the top, and spaced by 10 V. Overlaid are fits to the data described in the text.

asymmetry is not evident from inspection of the device. It is likely that with such asymmetry, the actual phase relation is indistinguishable from that of a tunnel junction.

4 Conclusion Measurement of the current–phase relation of graphene can give indication that electronic transport is ballistic. Distinctive, identifiable features are also present in the dc graphene SQUID critical current–flux dependence. Further work is necessary to produce devices with electrode separation L much less than the mean free path. Such devices will directly probe the nature of the "massless Dirac fermion" quasiparticles in graphene, instead of the coupled system of quasiparticles plus scatterers.

Acknowledgements This work was supported by the Director, Office of Energy Research, Office of Basic Energy Sciences, Materials Sciences and Engineering Division, of the US Department of Energy under contract DE-AC02-05CH11231 and the Office of Naval Research under grant N00014-07-1-0774. Y. Z. acknowledges a postdoctoral fellowship and V. B. a visiting professor fellowship from the Miller Institute, UC Berkeley.

References

[1] K. S. Novoselov, A. K. Geim, S. V. Morozov, D. Jiang, Y. Zhang, S. V. Dubonos, I. V. Grigorieva, and A. A. Firsov, Science **306**, 666 (2004).
[2] A. H. Castro-Neto, F. Guinea, N. M. R. Peres, K. S. Novoselov, and A. K. Geim, Rev. Mod. Phys. **81**, 109 (2009).
[3] J. H. Chen, C. Jang, S. Adam, M. S. Fuhrer, E. D. Williams, and M. Ishigami, Nature Phys. **4**, 377 (2008).
[4] X. Du, I. Skachko, A. Barker, and E. Andrei, Nature Nanotechnol. **3**, 491 (2008).
[5] K. I. Bolotin, K. J. Sikes, Z. Jiang, M. Klima, G. Fudenberg, J. Hone, P. Kim, and H. L. Stormer, Solid State Commun. **146**, 351 (2008).
[6] Y.-W. Son, M. L. Cohen, and S. G. Louie, Nature **444**, 347 (2006).
[7] B. Trauzettel, D. V. Bulaev, D. Loss, and G. Burkard, Nature Phys. **3**, 192 (2007).
[8] M. Titov and C. Beenakker, Phys. Rev. B **74**, 041401(R) (2006).
[9] A. A. Golubov, M. Yu. Kupranov, and E. Il'chev, Rev. Mod. Phys. **76**, 411 (2004).
[10] Ç. Ö. Girit, V. Bouchiat, O. Naaman, Y. Zhang, M. F. Crommie, A. Zettl, and I. Siddiqi, Nano Lett. **9**, 1 (2009).
[11] T. A. Fulton, L. N. Dunkelberger, and R. C. Dynes, Phys. Rev. B **6**, 855 (1972).